

# Structural Performance of 14m HAWT blade through CFD

Praveen Kumar Nigam, Nitin Tenguria, M. K. Pradhan



**Abstract:** An alternative method used in generating energy is with the help of wind turbines utilizing power from the winds. The efficient extraction of energy hinges on the geometry and structure of the blade. The blade of wind turbine encounters high operational loads and undergoes fluctuating conditions of environment. The proposed work comprises of creating an exact model using CAD applications which includes the optimized geometry of the blade in addition with process verification of structural integrity, under several operating conditions by the means of finite element analysis. The prime motive of the proposed study is to check and evaluate the reliability of the blades by developing the entire geometry of the blade and performing failure analysis by altering load conditions. The construction of blade geometry is done by implementing the blade element momentum theory (BEMT) in order to retrieve the ultimate power coefficient at the required tip speed ratio of 7.05 by the means of optimization process. The NACA 63(4)-221 airfoil is used to create the primary design of blade. Blade with 14 m length has been taken for the present work for RRB V27-225 kW HAWT (horizontal axis wind turbine blade), which is an exclusive design of the blade. In order to perform analysis and modeling of the blade in presence and absence of shear web, two individual materials such as carbon fiber and glass fiber are taken in account. In the case of carbon fibre with shear web, the structural strength is improved which is shown in the results.

**Index Terms:** Structural analysis, HAWT, CFD, ANSYS, Blade material, Shear web.

## I. INTRODUCTION

Wind turbines blades are made by various blade profiles. Since the chosen wind turbine belongs to a large size, hence structural analysis becomes important. This analysis has inclusions regarding creation of an accurate CAD model of new blade geometry which is optimized and verification process of structural integrity for the new blade under multiple conditions of operation using finite element analysis. The development of the complete blade structure and failure analysis after application of different loading conditions to verify the reliability of wind turbine blades is the primary objective of this section.

Revised Manuscript Received on January 30, 2020.

\* Correspondence Author

Praveen Kumar Nigam\*, Rabindranath Tagore University, Raisen, 464993, India. nigam.praveen@gmail.com

Nitin Tenguria, Sagar Institute of Research & Technology, Bhopal, 462041, India. tengurianitin@gmail.com

M. K. Pradhan, Maulana Azad National Institute of Technology Bhopal, 462003, India. mohanrkl@gmail.com

© The Authors. Published by Blue Eyes Intelligence Engineering and Sciences Publication (BEIESP). This is an open access article under the CC-BY-NC-ND license <http://creativecommons.org/licenses/by-nc-nd/4.0/>.

## II. LITERATURE SURVEY

Blades are the most important part of wind turbines, which play a significant role in energy efficiency. The repeated failures in blade could be costly; therefore regular monitoring of the blades provides substantial benefits. Turnbull and Omenzetter proposed a new application of FFEMU (Fuzzy Finite Element Model Updating) of wind turbine blades for the evaluation of the structural condition of blade. Experimental based frequencies comprising blade of small scale wind turbine is defined by the means of Modal analysis. Fuzzy numbers are used to identify the frequencies in measurement of uncertainty in the model. A non-destructive way was introduced by adding small mass on the trailing edge of the blade that can induce a structural change and then simulation are conducted. This technique was found beneficial for the extent of effective modification as well as to detect the location [16].

Zhang et al. carried out the structural collapse test on a wind turbine blade with blade length of 52.5m under the condition of combined load. The complete track of action of damage under the ultimate load was analyzed. The analysis shows nonlinear buckling of the shear web as well as spar cap. This results irregular distribution of stress, further fracture of aft panel, which ultimately leads to severe damage on the turbine blades. Conclusions drawn shows that the debonding on trailing edge and delamination of aft panel has major impact for severe failures of the blade. [18]

Smith et al. performed aero hydro structural analysis on a wind turbine located offshore with the capacity of 5MW. Analysis is performed in order to achieve maximum safety in the base design, and interaction of structure of soil under complex aero hydro loading. The monopile foundation design developed by the NREL was chosen for the study. The loadings on the foundation such as aerodynamic as well as hydrodynamic were simulated using high fidelity method on CFD under varying flow conditions. Further, in order to evaluate the stress field of the foundation along with the soil, the structural dynamic analysis was performed. In the monopile foundation for the stress field, the Morison equation is conservative as indicated by the results, whereas it is underestimated in the soil [14]

Mouhsine et al. developed structure of airfoil in order to get optimum shape of blade of NREL phase 2 and phase 3 horizontal axis wind turbine (HAWT). Firstly airfoils characteristics were chosen, and then using BEMT primary blade design was identified. The sections of airfoil used were S818, S825 and S826.

The coordinates of the blade were generated using MATLAB code. Then structural analysis and aerodynamic analysis were carried out. Commercial software Fluent was utilized to generate flow field and perform calculations using RANS (Reynolds-averaged Navier Stokes) with incorporation of FEM based k-omega SST model [10].

Mathew et al. researched on five individual materials for blade, such as Epoxy carbon, Structural steel, E-glass, S-glass and Aluminium alloy. The model of the blade was created using CATIA V5 which is commercial software. Further, analysis was carried out on the same model using ANSYS which also comes under commercial software. Hence, the work on the wind turbine blade was explored using finite element analysis. The key objective of the research was to validate the mechanical properties of the wind turbine blade and further compare all the five materials to identify most suitable material for the blade. The analysis results showed the blade comprising epoxy carbon material had the best mechanical properties among the five [1]. Zhu et al. investigated the effect of blade flexibility on wind turbine loads and power production. Hence, a developed aeroelastic model was created. The aerodynamic loads were evaluated by developing a free wake vortex lattice model. To calibrate the structural dynamics of the blade, theory of exact beam geometry was adopted. The reference model of the wind turbine blade was taken from the National Renewable Energy Laboratory (NREL) 5MW. A marginal deduction in the rotor power was observed at high speed of wind considering the flexibility of the blade. Setting up the pitch angle at lower value helps to maintain a consistent rotor power at elevated wind speeds [19].

Sener et al. (2018) researched the impact of fiber orientation angle of spar cap of composite blades having IBTC (induced bending torsion coupling) on the aero-structural performance of wind turbines. IBTC blades along with aero-structural performance was evaluated with mitigation of fatigue load in the complete turbine system, clearance tower, peak stresses in the blades and generation of power from the wind turbine. A blade made of E-glass/epoxy with novel and IBTC, a hybrid E-glass/carbon/epoxy blade with IBTC were designed. Further, multibody simulations of 5MW turbine system having aeroelastic time-marching were done with the blades of IBTC and the reference blade model comprising a total of six randomly generated turbulent wind profiles. Fatigue-equivalent loads (FELs) comprising the wind turbine was determined from the average of the time response results obtained from six different simulations. The results show that specific hybrid blade designs with IBTC are more active in mitigating fatigue loads compared to the composite blade with E-glass/epoxy with IBTC. Moreover, the orientation angle of fiber and sectional properties of hybrid blades must be calibrated accordingly utilizing multiple layers of carbon/epoxy within the sections of the blade with IBTC to minimize losses of generator power and FEL [13].

A windmill blade bear high operating loads and undergoes several impacts from the environment which results in failure due to penetration of fatigue, defects and damage due to weather conditions. A distinctive and acoustic based health monitoring and structural sensing system is developed, which requires effective algorithms to identify the damage in

operating cavity structures. Regan et al. described the selection of a set of statistical features in order to identify the damage on closed cavities based on acoustics. Identification of SVM as well as LR was along with the usage of optimal feature selection for making the decision with the help of binary classification algorithms. For damage detection studies, a laboratory-scale wind turbine was built to comprising of hollow composite blades [11].

Since, there is rapid development in high end performing devices and computational sources; Navier-Stokes computational fluid dynamics (CFD) proposes an accurate as well as cost effective way to improve the comprehension regarding unsteady aerodynamics of wind turbines so as to offer more effective designs. In this framework, Balduzzi et al. has done the investigation comprehensively on the 3D unsteady aerodynamics in Darrieus-like motion on a single blade, along with the time-dependent 3-D Navier Stokes simulations was conducted on an IBM BG/Q cluster with more than 16,000 processor cores per simulation. Special attention was given on tip losses, dynamic stall, and wake interaction. The results obtained by CFD simulations were compared with results obtained with the Lifting Line Free Vortex Wake Model (LLFVW) based on an open-source code. This method is most robust technique among the models of “lower-fidelity”. Additionally, since the wake clearly gets resolved in comparison to methods based on BEM, LLFVW incorporates three dimensional flow solutions on analysis. Comparison amongst these methods was done and critical analysis was carried out to identify their merits and de-merits [5].

Bagherpoor and Xuemin offered a process based MATLAB code needed for structural optimization of blades of wind turbines. Material selection from composites offers more flexible, lighter and stronger blades. Structural analysis was carried out on horizontal-axis wind turbine blade with blade length 82 meter. A preliminary tool was incorporated for analysis and structural optimization that was capable to design and evaluate the composite layups and analyse the impact on the properties of the composite blade. [4]

A thorough and combined study needs to be done on rotational motion of rotor and vibration of blade while modelling wind turbine blade. Ju and Sun developed a dynamics model of a rotational rotor of a HAWT by the means of Lagrange’s approach and finite element methods, which explains the terms of coupling among the gross rotation of the rotor and blade elastic movement. The new model developed was further validated by a model created in commercial software FAST. The results showed that impact of coupling can elevate the sensitivity in methods implemented to identify faults from blades. The depicted model can also be utilized to analyse the impact of different terms in addition with analysis of fluid structure interaction. [9].

The purpose of aeroelastic tailoring is to improve the ratio between mass and power capture, by the means of system durability and enhanced combined energy capture. Scott et al. assumed two adaptive wind turbine blades which were aeroelastically tailored.

The initial uses material bend-twist coupling, while the other one uses both material and geometric bend twist coupling. The performance parameters of the turbine system were evaluated and compared in terms of pitch, load, and pitch rate. Lastly, decreases in pitch rate along with the power smoothing abilities were shown by the adaptive blades.

Although, the increased pitch rate in blade root torsional moment probably benefits the pitch system. For optimization as well as analysis of wind turbines, an accurate along with a fast calculation of structural properties has been required by multiple engineering applications [12].

Ashuri and Zhang provided "CompSim", an open-source computational code so as to construct structural properties of complicated geometries comprised of materials which are inhomogeneous. Investigation of properties such as mass distribution, stiffness coefficients along with the moment of inertia was carried out using weighted average method. In order to analyse the accuracy of the code, a 20 MW wind turbine model was selected for computation from general research. This code is useful in developing and optimizing in a preliminary design phase for further analysis [3].

Thomas et al. presented spar with I shaped section known to be most essential part of wind turbine blade for bearing the load. I shape spar was compared with traditional box-type spar using FEM analysis. The study was performed on blade profile S810 in the flap wise direction. The performance of the blade was also compared with two diverse materials that are carbon fiber and epoxy fiber. It was concluded that carbon fiber provides better performance and can withstand higher loads [15].

The material selection regarding blades is crucial for better operation of wind turbines. The challenges are related to the optimum combination of the rigidity, specific gravity, fatigue, flexibility, cost of materials and processing to achieve the desired aerodynamic shape. Domnica et al. worked on the identification of risk areas of wind turbine blades and composite structural optimization on combined loading using finite element analysis. For analysis, blade length was taken 1.5 m and profile NACA 2412 made by composite fiber-reinforced polymer with layers of fiberglass fabric and mat with epoxy resin as the matrix. Then in the next stage, structural verification, as well as optimization, was performed. It was concluded that, as the number of layers increases in the risk areas, it leads to increased resistance to static and dynamic loads. The orientation of layers can improve the dynamic as well as static behaviour [7].

Due to several layers of composite materials and various components like shear webs etc., a wind turbine blade has a challenging design structure. Wang et al. developed model for structural optimization regarding composite blades based on the models of genetic algorithm and finite element analysis. The objective of the optimization model was to eliminate the mass of composite blades having multi-criteria constraints, for example, continuity of laminate layups, along with the manufacturing maneuverability, buckling, including deformation as well as stress. The design variables selected were, number of unidirectional plies in addition with the locations of the spar cap and the shear web thickness. The complete arrangement was applied on ELECTRA 30kW vertical axis wind turbine. As compared to the initial design weight which is 228kg, the optimized blade has achieved

17.4% lower weight [17].

High-intensity wind can be a danger to the structural integrity of wind turbines. Chen and Xu proposed a failure structural analysis of damaged wind turbine by Usagi, a super typhoon in 2013. The collapse of tower, along with the substantial variation in the direction of the wind on fracture, including the effect of high-intensity wind was aimed as a special focus for the research. Investigation at field and information regarding local winds were collected and analyzed. Through structural modeling as well as integrating wind load calculation, a systematic procedure was developed. To determine the root cause of failure, quantitative based research was carried out on structural response on the rotor blades and the tower of wind turbine. Under typhoon or hurricane-like extreme wind conditions, to minimize the risk of wind turbine failure, some direction of modification of the current IEC design has been proposed in this study. [6].

In present work, the construction of blade geometry is done by the process of optimization in order to achieve maximum power coefficient at the desired tip speed ratio of 7.05 by implementation of blade element-momentum theory (BEMT). The structure of the blade is primarily designed using NACA 63(4)-221 airfoil. The structure of blade is designed using BEMT to calculate the conditions of load at different inflow velocities. Selection of vertical shear web is done to produce in the structural grid of the blade. Further, high-strength unidirectional fibers of E-glass and carbon materials are selected to design the blade. The final structure of blade is then analysed using the finite element method in ANSYS Workbench. The results depicted that, the proposed blade structure can withstand the applied loads.

### III. BASIC STEPS TO PERFORM FINITE ELEMENT ANALYSIS

#### A. Pre-processing

**CAD Modelling:** Generating CAD model with help of CAD modelling tools for creating the geometry of the part/assembly for FEA implementation

**Meshing:** In FEA, meshing is a critical operation. The operation divides the complete geometry in a number of small pieces. These small pieces are termed as mesh. The accuracy of analysis depends on the size of mesh and its orientation. The finite element analysis speed increases when there is an increase in mesh size however the accuracy decreases. Meshing includes the following Steps.

- **Element Selection:** As per the dimensionality such as, 1-dimensional, 2-dimensional or 3-dimensional, elements are selected.
- **Mesh Type:** A huge geometric domain is indicated by a mesh with small discrete cells. To compute solutions, meshes are generally taken in usage to analyze geographical and cartographic data, as well as to render computer graphics, together with partial differential equations. The partition space of mesh comprised of elements or cells. Cell shape can be a triangle and the quadrilateral under 2D type. The primary 3D elements are tetrahedron, quadrilateral pyramid, triangular prism, and hexahedron.

- **Defining Material Properties:** It is important to define the FEA package regarding the material selection for each part. Through this process, details regarding modulus of elasticity, along with the Poisson's Ratio as well as all other necessary properties are mandatory which are required for the FEA.
- **Mesh Size:** Describe the size of mesh that includes no. of division along with the element edge length.
- **Generation of the mesh:** Depending on given variables, the mesh is generated.

**B. Defining Boundary Condition & loading**

The boundary includes assignment of known value for a displacement or any related load conditions. These conditions determine the surrounding conditions of the model in terms of loads and constraints.

**C. Results or Solution**

In this step, boundary conditions, mesh size and material properties are defined to the FEA package and result is achieved.

**D. Post-processing**

In this step, interpretation as well as viewing of results is done. Several formats are available for viewing the results such as: contours, graph, value, animation, etc.

**IV. FINITE ELEMENT ANALYSIS OF BLADE USING ANSYS**

**A. Pre-processing**

**CAD Model:** Firstly CAD model of NACA airfoil 63(4)-221 is prepared using given coordinates in Table- II. As the blade is divided into 10 elements and twisted differently at each section as well as reduced chord length towards the tip of the blade. Fig. 1 and 2 show side and front view of sections of the blade according to data of chord length and twist angle is given in Table- III below. A number of parameters have been listed in Table- I. Fig. 3 to 6 shows the wireframe and surface model of the blade with and without shear webs.

**TABLE- I. Parameters for CAD model of blade**

Length of blade	14 m
Chord length (maximum)	1.3648 m
Chord length (minimum)	0.5461 m
Type of airfoil	NACA 63(4)-221

**TABLE- III. Chord length and twist angle at each element for TSR = 7.05**

Element number	Radius, r (m)	Chord length, (m)	Thickness of airfoil, (m)	Twist angle, $\theta'$ (degree)
1	1.4	1.3648	0.2866	41.18
2	2.8	1.2738	0.2675	33.26
3	4.2	1.1829	0.2484	26.18
4	5.6	1.0919	0.2293	19.94
5	7.0	1.0009	0.2102	14.53
6	8.4	0.9100	0.1911	09.95
7	9.8	0.8190	0.1720	06.20
8	11.2	0.7281	0.1529	03.28
9	12.6	0.6371	0.1338	01.20
10	14.0	0.5461	0.1147	-0.04

**TABLE- II. Airfoil specification of NACA 63(4)-221**

Upper surface		Lower surface	
Station	Ordinate	Station	Ordinate
0.00000	0.00000	0.00000	0.00000
0.00367	0.01627	0.00633	-0.01527
0.00600	0.02001	0.00900	-0.01861
0.01075	0.02628	0.01425	-0.02414
0.02292	0.03757	0.02708	-0.03385
0.04763	0.05375	0.05237	-0.04743
0.07253	0.06601	0.07747	-0.05753
0.09753	0.07593	0.10247	-0.06559
0.14767	0.09111	0.15233	-0.07765
0.19792	0.10204	0.20208	-0.08612
0.24824	0.10946	0.25176	-0.09156
0.29860	0.11383	0.30140	-0.09439
0.34897	0.11529	0.35103	-0.09469
0.39934	0.11369	0.40066	-0.09227
0.44969	0.10949	0.45031	-0.08759
0.50000	0.10309	0.50000	-0.08103
0.55027	0.09485	0.54973	-0.07295
0.60048	0.08512	0.59952	-0.06370
0.65063	0.07426	0.64937	-0.05366
0.70071	0.06262	0.69929	-0.04318
0.75073	0.05054	0.74927	-0.03264
0.80067	0.03849	0.79933	-0.02257
0.85056	0.02693	0.84944	-0.01347
0.90039	0.01629	0.89961	-0.00595
0.95018	0.00708	0.94982	-0.00076
1.00000	0.00000	1.00000	0.00000

LE Radius: 0.0265, slope of radius through LE 0.0842



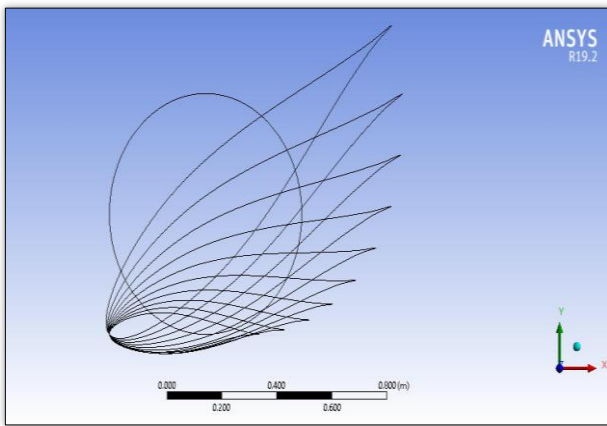


Fig. 1. Setting up airfoils at different twist angle at fixed element size (side view)

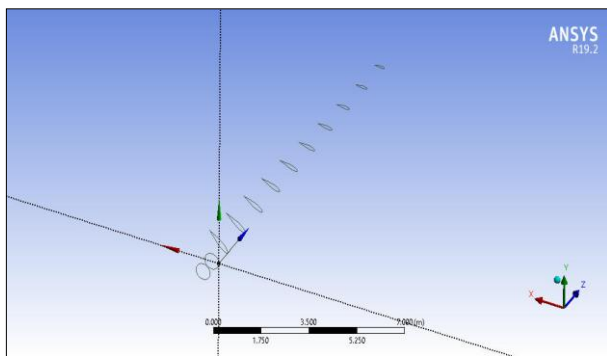


Fig. 2. Setting up airfoils at different twist angle at fixed element size (front view)

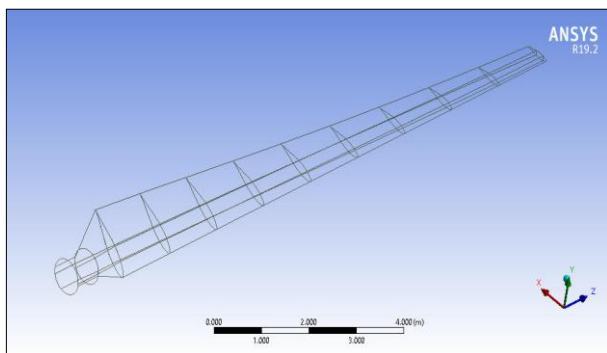


Fig. 3. Wireframe geometry of blade without shear web

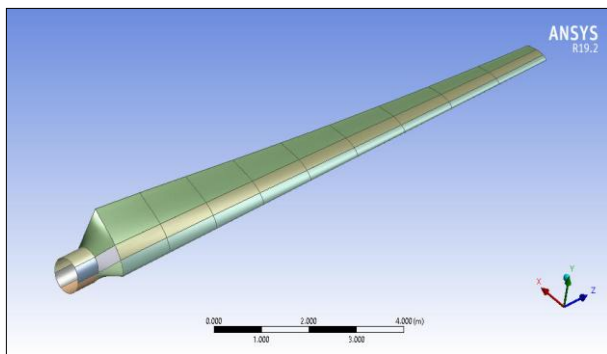


Fig. 4. Surface model of blade without shear web

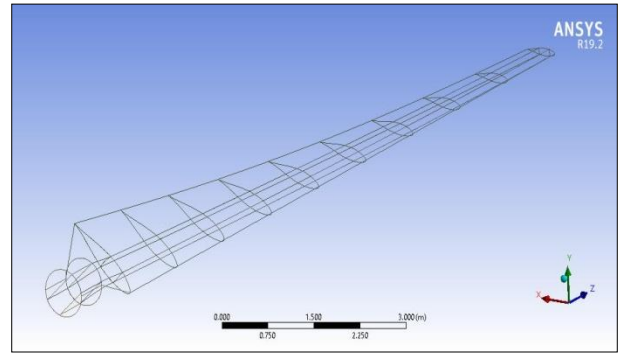


Fig. 5. Wireframe geometry of blade with shear web

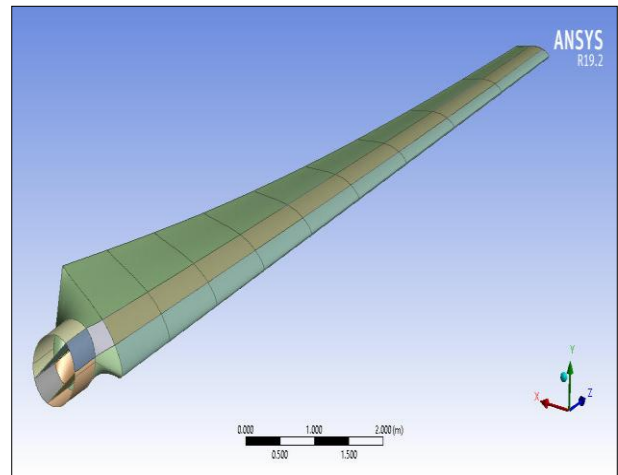


Fig. 6. Surface model of blade with shear web

### Meshing

- **Element selection:** The selection of element type is a 3-D shell element for the purpose of meshing.
- **Mesh type:** A huge geometric domain is indicated by a mesh with small discrete cells. Quadrilateral mesh type was used for meshing. This cell shape is a basic 4 sided and most common in structured grids.
- **Element type:** For the meshing of the blade surface, 4 Node shell element has been taken in account. Four nodes are defined by the elements with six degrees of freedom at every node. The element also defines translation and rotation in directions x, y and z axes.
- **Define the material properties of the blade:** Two materials are taken for comparison purpose to achieve better strength. Table-IV shows the different properties of the selected material for the blade.
- **Mesh Size:** Mesh size is defined by specifying element edge length, a number of nodes, and a number of elements. Table-V shows Input parameters related to mesh size for the meshing of the blade.
- **Generation of the mesh:** Meshing was created using parameter specifies from Table-I to V. Fig. 7 to 9 shows meshing of the blade with and without shear web.

TABLE- IV. Material properties of blade

Material type	Young's modulus, E, (Mpa)	Poisson's ratio	Tensile strength, (Mpa)	Density, (kg/m <sup>3</sup> )
E-Glass fibre reinforced plastic	38000	0.2	1800	1870
Carbon fibre reinforced plastic	176000	0.27	2050	1490

TABLE- V. Input parameters for meshing of blade

S. No.	Parameters	For blade without shear web	For blade with shear web
1	Element Edge Length	20 mm	20 mm
2	No. of Nodes	51603	64823
3	No. of Element	51568	63448

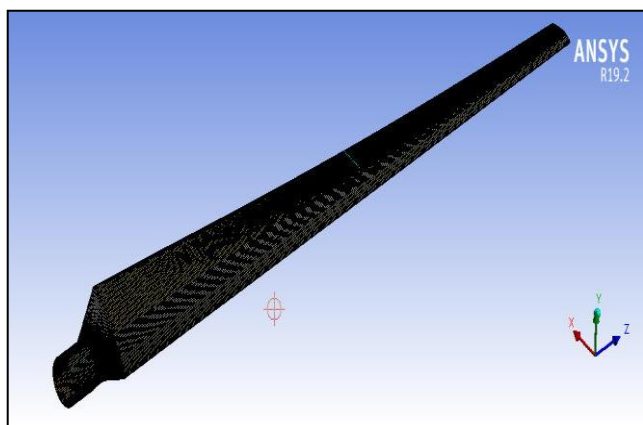


Fig. 7. Meshing of blade structure without shear webs

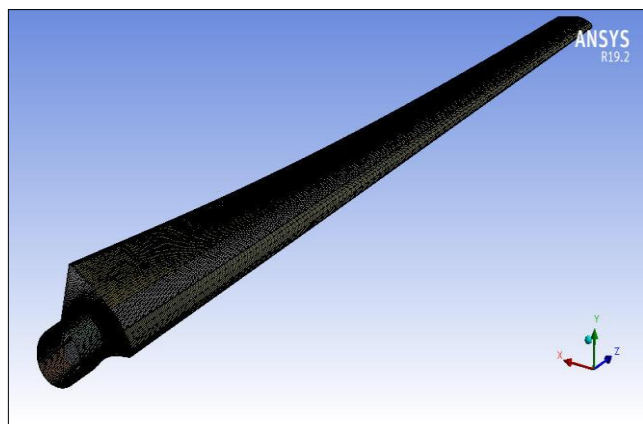


Fig. 8. Meshing of blade structure with shear webs

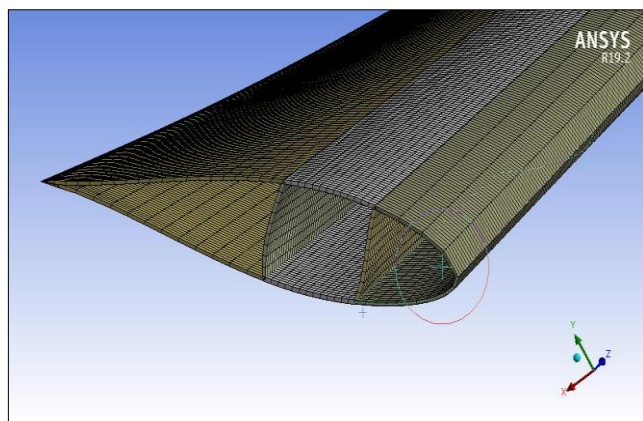


Fig. 9. Meshing of blade structure with shear webs (section view)

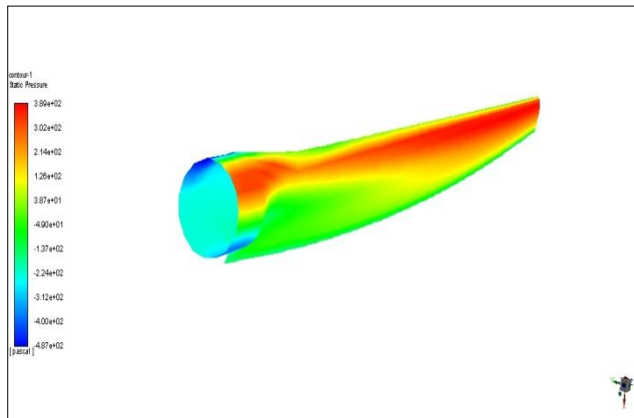


Fig. 10. Three dimensional view of pressure distribution on blade at velocity = 24m/s

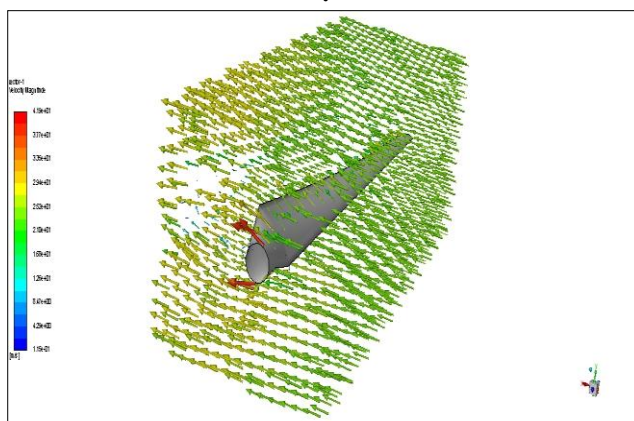


Fig. 11. Three dimensional view of vector representation on blade at velocity = 24m/s

**B. Boundary condition and Loading**

- **Boundary condition:** One end is kept fixed at the root of the blade and free at another end.
- **Load:** (a) Wind pressure from CFD analysis of blade at a wind speed of 24 m/s applied at the surface of the blade. (b) Gravity due to self-weight is also considered.

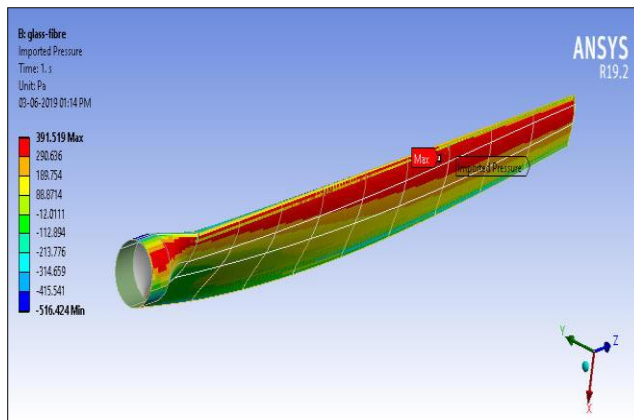


Fig. 12. Applying pressure load on blade structure

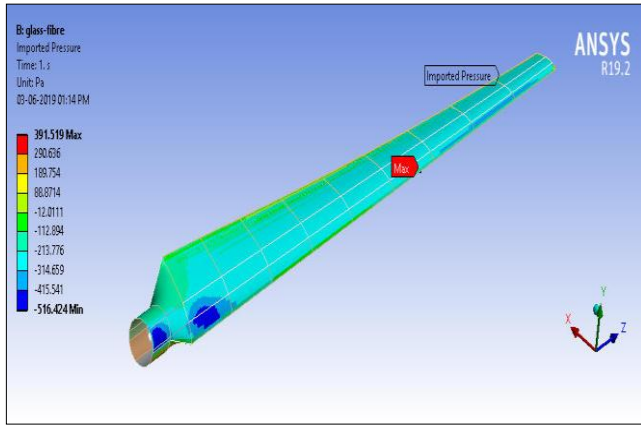


Fig. 13. Applying imported pressure load from CFD analysis

V. RESULTS

In this step, ANSYS solve the problem for mesh size, as well as a boundary condition, along with the defined material properties. Fig. 12, 15, 18, and 21 show the contour of deformation distribution along the blade with and without the shear web of material glass fiber and carbon fiber. While Fig. 13, 14, 16, 17, 19, and 20 shows the distribution of von-mises stress along the blade with and without the shear web for material glass fiber and carbon fiber.

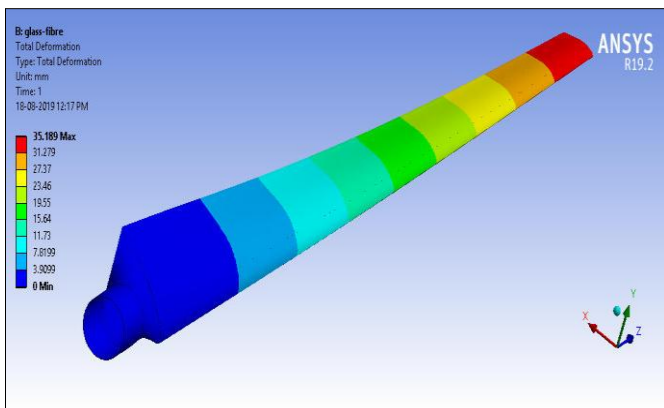


Fig. 14. Contour of deformation distribution along blade without shear web of glass fibre

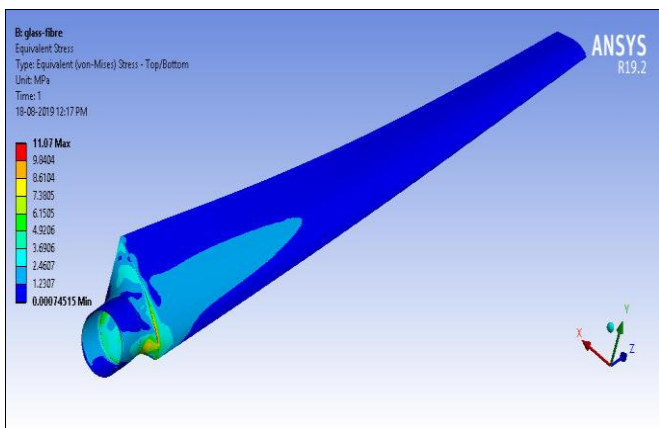


Fig. 15. Distribution of von-mises-stress along the blade without shear web (glass fibre)

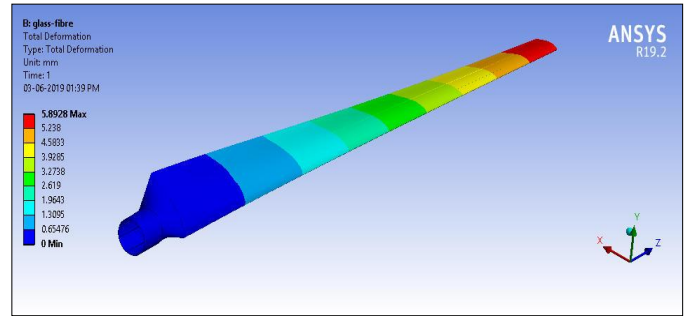


Fig. 16. Contour of deformation of blade with shear web (glass-fibre)

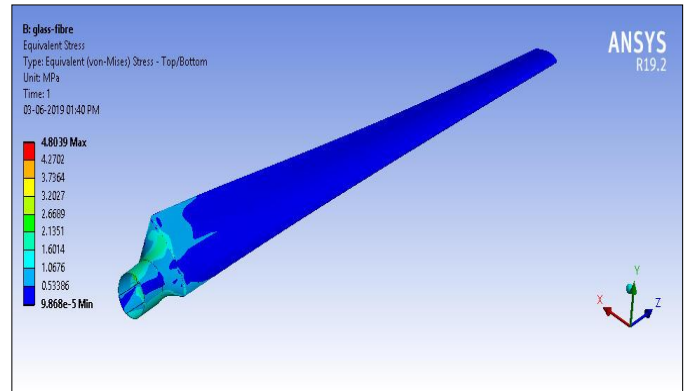


Fig. 17. Distribution of von-mises-stress along the blade with shear web (glass fibre)

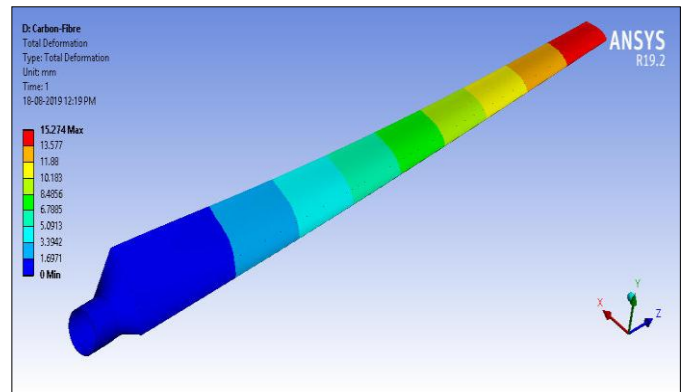


Fig. 18. Contour of deformation of blade without shear web (carbon-fibre)

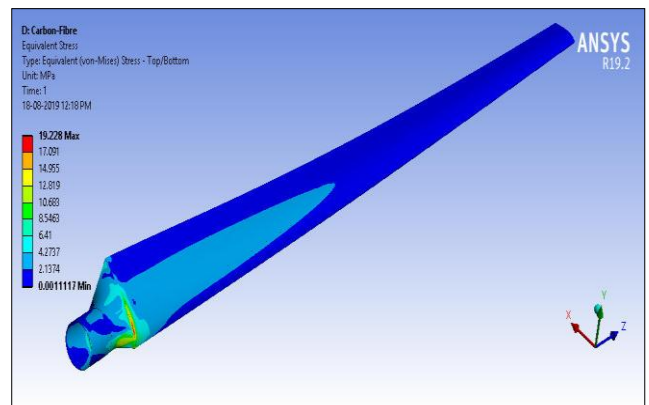
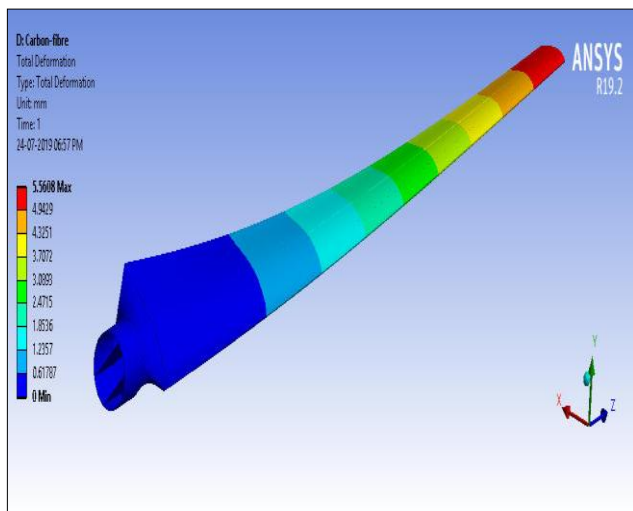
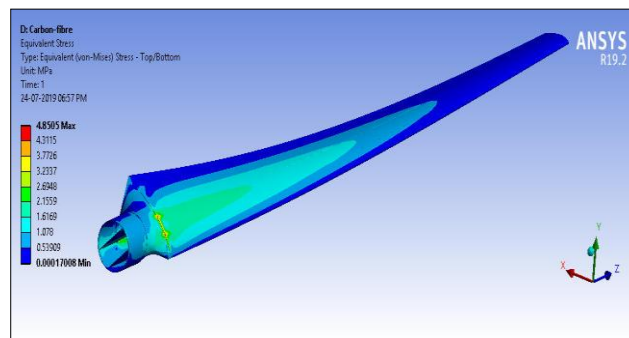


Fig. 19. Distribution of Von-Mises-Stress along the blade without shear web (carbon fibre)



**Fig. 20. Contour of deformation of blade with shear web (carbon-fibre)**



**Fig. 21. Distribution of Von-Mises stress along the blade with shear web (carbon fibre)**

**A. Post Processing**

For interpretation as well as viewing of the result of the above-solved problem. The results obtained can be observed in different formats such as data, graph, animation etc. Table-VI shows the result of structural analysis of the blade of material glass fiber and carbon fiber with and without the shear web.

Table-VI shows deformation at a different section of the blade for glass fiber and carbon fiber with and without the shear web. Fig. 21 shows the graph for the same. Table-VII shows von mises stress at a different section of the blade for glass fiber and carbon fiber with and without shear web. Fig. 22 shows the graph for the same.

**TABLE- VI. Result of structural analysis of blade with glass fibre and carbon fibre materials**

Blade material	Structure	Wind speed (m/s)	Average pressure on blade (Pa)	Weight (kg)	Maximum deformation (mm)	Von-mises stress (Mpa)	Nodes	Element
Glass fibre reinforced plastic	Without shear web	24	55.1548	559.39	35.189	11.07	51603	51568
Glass fibre reinforced plastic	With shear web	24	55.1548	699.77	5.8928	4.8039	64823	63448
Carbon fibre reinforced plastic	Without shear web	24	55.1548	445.72	15.274	19.228	51603	51568
Carbon fibre reinforced plastic	With shear web	24	55.1548	557.57	5.5608	4.8505	64823	63448

**TABLE- VII. Deformation of blade for glass fibre and carbon fibre with and without shear web**

S. No.	Deformation of blade (glass fibre without shear web), (mm)	Deformation of blade (glass fibre with shear web), (mm)	Deformation of blade (carbon fibre without shear web), (mm)	Deformation of blade (carbon fibre with shear web), (mm)
1	0.000	0.000	0.000	0.000
2	3.9099	0.6547	1.6971	0.6178
3	7.8199	1.3095	3.3942	1.2357
4	11.730	1.9643	5.0913	1.8536
5	15.640	2.6190	6.7885	2.4715
6	19.550	3.2738	8.4856	3.0893
7	23.460	3.9285	10.183	3.7072
8	27.370	4.5833	11.880	4.3251
9	31.279	5.2380	13.577	4.9429
10	35.189	5.8928	15.274	5.5608

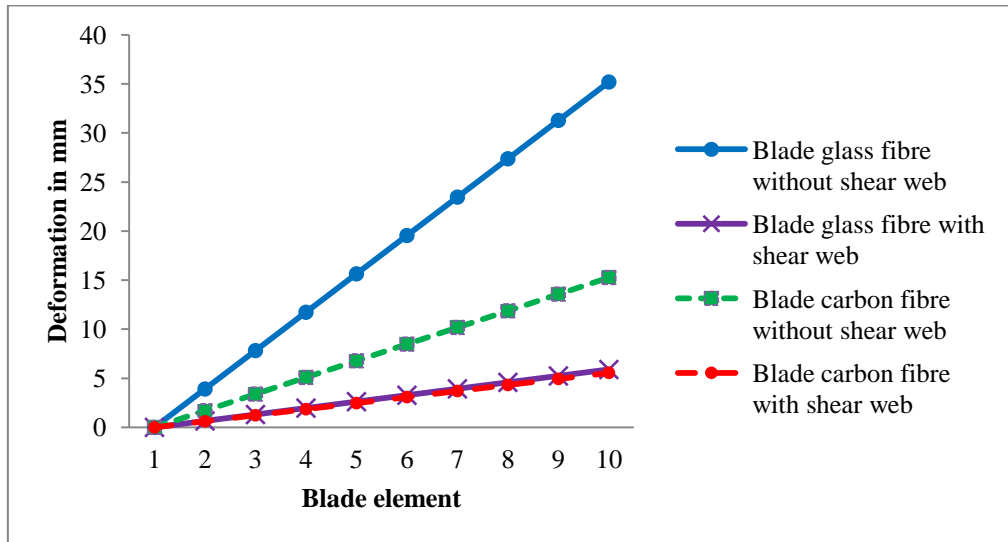


Fig. 22. Deformation at different section of blade with and without shear web for glass fibre and carbon-fibre

TABLE- VIII. Von Mises Stress of blade for glass fibre and carbon fibre with and without shear web

S. No.	Von mises stress (Glass fibre without shear web)	Von mises stress (Glass fibre with shear web)	Von mises stress (Carbon fibre without shear web)	Von mises stress (Carbon fibre with shear web)
1	0.00074515	0.00009868	0.0011117	0.00017008
2	1.2307	0.53386	2.1374	0.53909
3	2.4607	1.0676	4.2737	1.078
4	3.6906	1.6014	6.4100	1.6169
5	4.9206	2.1351	8.5463	2.1559
6	6.1505	2.6689	10.683	2.6948
7	7.3805	3.2027	12.819	3.2337
8	8.6104	3.7364	14.955	3.7726
9	9.8404	4.2702	17.091	4.3115
10	11.070	4.8039	19.228	4.8505

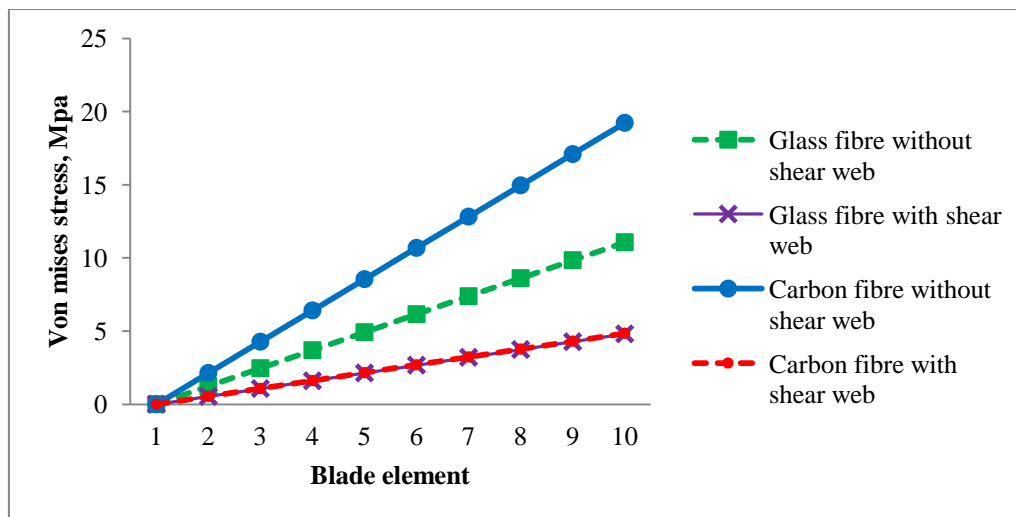


Fig. 23. Von Mises stress at different section of blade with and without shear web for glass fibre and carbon-fibre

VI. CONCLUSION

Results shows maximum deformation distribution along blade made by glass fibre without shear web is 47.606 at tip and average value 23.80 mm throughout the blade. The same blade material with shear web shows maximum deformation 5.8928 mm at tip and average value 2.9463 mm. The deformation distribution along blade made by carbon fibre

without shear web is 18.156 mm at tip and average value 9.0779 mm along the blade, while the same blade with shear web shows maximum deformation 5.5608 mm at tip and average value 2.7803 mm. It is clearly shown that providing shear web give drastic decrement in maximum and average deformation of blade.

Results also shows maximum von mises stress distribution along blade made by glass fibre without shear web is 19.509 MPa at tip and average value 9.7551 MPa throughout the blade. The same blade material with shear web shows maximum von mises stress 4.8039 MPa at tip and average value 2.4020 MPa. The von mises stress distribution along blade made of carbon fibre blade without shear web is 38.538 MPa at near tip and average value 19.2694 MPa along the blade, while the same blade with shear web shows maximum stress 4.8505 MPa at tip and average value 2.4253 MPa. It is clearly shown that providing shear web give drastic decrement in maximum and average stress of blade. It is obvious from results that carbon fibre material shows light weight and better strength than glass fibre. Both materials show safe under specified boundary conditions.

### ACKNOWLEDGMENT

The authors would like to acknowledge the research support from the Rabindranath Tagore University, Bhopal, India.

### REFERENCES

1. Akhil P Mathew, Athul S, Barath P and Rakesh S., Structural analysis of composite wind turbine blade. International research journal of engineering and technology, 05(06), 2018, pp 1377-1378
2. Alom, N. and Saha, U., Evolution and progress in the development of savonius wind turbine rotor blade profiles and shapes, Journal of solar energy engineering, 2018, 141(3).
3. Ashuri, T. and Zhang, J., CompSim: Cross sectional modeling of geometrical complex and inhomogeneous slender structures, SoftwareX, ScienceDirect, 6, 2017, pp.155-160.
4. Bagherpoor, T. and Xuemin, L., Structural optimization design of 2mw composite wind turbine blade, Energy Procedia, 105, 2017, pp.1226-1233.
5. Balduzzi, F., Marten, D., Bianchini, A., Drofelnik, J., Ferrari, L., Campobasso, M., Pechlivanoglou, G., Nayeri, C., Ferrara, G. and Paschereit, C., Three-dimensional aerodynamic analysis of a Darrieus wind turbine blade using computational fluid dynamics and lifting line theory, Journal of engineering for gas turbines and power, 2017, 140(2).
6. Chen, X. and Xu, J., Structural failure analysis of wind turbines impacted by super typhoon Usagi, Engineering failure analysis, 60, 2016, pp.391-404.
7. Domnica, S., Ioan, C. and Ionut, T., Structural optimization of composite from wind turbine blades with horizontal axis using finite element analysis, Procedia technology, 22, 2016, pp.726-733.
8. Eggleston, D. and Stoddard, F., Wind turbine engineering design, New York: Van nostrandreinhold, (1987)
9. Ju, D. and Sun, Q., Modeling of a Wind Turbine Rotor Blade System. Journal of vibration and acoustics, 2017, 139(5).
10. Mouhsine, S., Oukassou, K., Ichenial, M., Kharbouch, B. and Hajraoui, A., Aerodynamics and structural analysis of wind turbine blade, Procedia Manufacturing, 22, 2018, pp.747-756.
11. Regan, T., Beale, C. and Inalpolat, M., Wind turbine blade damage detection using supervised machine learning algorithms, Journal of vibration and acoustics, 2017, 139(6).
12. Scott, S., Capuzzi, M., Langston, D., Bossanyi, E., McCann, G., Weaver, P. and Pirrera, A., Effects of aeroelastic tailoring on performance characteristics of wind turbine systems, Renewable energy, 114, 2017, pp.887-903.
13. Sener, O., Farsadi, T., OzanGozcu, M. and Kayran, A., Evaluation of the effect of spar cap fiber angle of bending–torsion coupled blades on the aero-structural performance of wind turbines. Journal of solar energy engineering, 2018, 140(4).
14. Smith, S., Syed, A., Liu, K., Yu, M., Zhu, W., Huang, G., Chen, D. and Aggour, M., A comprehensive aero-hydro-structural analysis of a 5 MW offshore wind turbine system, Journal of solar energy engineering, 2019, 141(6).
15. Thomas, T., Narkhede, M., Patil, B. and Mogra, A., Analysis of wind turbine blade having I shaped spar using both epoxy fiber and carbon fiber using FEM, Materials today: proceedings, 4(2), 2017, pp.2573-2579.
16. Turnbull, H. and Omenzetter, P., Fuzzy finite element model updating of a laboratory wind turbine blade for structural modification detection, Procedia Engineering, 199, 2017, pp.2274-2281.
17. Wang, L., Kolios, A., Nishino, T., Delafin, P. and Bird, T., Structural optimisation of vertical-axis wind turbine composite blades based on finite element analysis and genetic algorithm. Composite structures, 153, 2016, pp.123-138.
18. Zhang, L., Guo, Y., Wang, J., Huang, X., Wei, X. and Liu, W., Structural failure test of a 52.5 m wind turbine blade under combined loading. Engineering failure analysis, 103, 2019, pp.286-293.
19. Zhu, X., Chen, J., Shen, X. and Du, Z., Impact of blade flexibility on wind turbine loads and pitch settings. Journal of solar energy engineering, 2019, 141(4).

### AUTHORS PROFILE



**Praveen Kumar Nigam**, is pursuing Ph.D. from Rabindranath Tagore University, Raisen, India. He completed his Master of Technology in Product Design and Engineering from Barkatullah University, Bhopal, India. His research interest is in development of renewal energy technologies and material science



**Dr. Nitin Tenguria**, received M. Tech. and Ph.D. from National Institute of Technology, Bhopal, India in 2007 and 2012. He is a Head in the Department of Mechanical Engineering, Sagar Institute of Research & Technology, Bhopal, India. He has more than 10 years of experience in teaching and research. His current area of research includes Wind Turbine blade.



**Dr. M. K. Pradhan**, is Assistant Professor in the Department of Mechanical Engineering, and Head of Production Engineering Lab. & Computer aided Manufacturing lab of the Maulana Azad National Institute of Technology, Bhopal, India. He received his M. Tech and Ph.D. in Mechanical Engineering from National Institute of Technology, Rourkela, India. He has over 15 years of teaching and research experience in manufacturing and 5 years of postdoctoral research experience in modeling and optimization of EDM processes.